Journal of Catalysis **207,** 286–295 (2002)
doi:10.1006/jcat.2002.3513, available online at http://www.idealibrary.com on IDEAL®

Hydrogenation of Cyclohexene over *in Situ* Fluorinated NiMoS Catalysts Supported on Alumina and Silica–Alumina

Lianglong Qu and Roel Prins[1]

Laboratory for Technical Chemistry, Swiss Federal Institute of Technology (ETH), 8093 Zurich, Switzerland

Received September 3, 2001; revised January 7, 2002; accepted January 12, 2002

The effect of fluorine on the hydrogenation of cyclohexene over sulfided NiMo catalysts supported on Al_2O_3 and amorphous silica–alumina (ASA) was studied at 5.0 MPa and between 310 and 350°C. Fluorination was performed *in situ* after sulfidation of the catalyst. The hydrogenation of cyclohexene produced mainly cyclohexane over the Al_2O_3-supported catalysts. On the ASA-supported catalysts, large amounts of the isomerization products methylcyclopentene and methylcyclopentane were formed in addition to the hydrogenation product cyclohexane. At the applied partial pressure of cyclohexene between 16 and 100 kPa, the hydrogenation is between zero and first order in the partial pressure of cyclohexene on all catalysts. The Al_2O_3-supported catalysts showed higher conversions of cyclohexene than their ASA-supported counterparts. Fluorination mainly enhances the isomerization of cyclohexene to methylcyclopentene. Kinetic parameters were obtained by fitting the kinetic data with Langmuir–Hinshelwood rate equations in a wide range of conversions. The unchanged activation energy and heat of adsorption for the hydrogenation of cyclohexene to cyclohexane indicate that the active sites for hydrogenation are not influenced by *in situ* fluorination. The activation energy for the isomerization of cyclohexene remained constant after fluorination. *In situ* fluorination introduces more acid sites for the isomerization reaction over both the Al_2O_3- and ASA-supported catalysts. © 2002 Elsevier Science (USA)

Key Words: **hydrogenation; cyclohexene; methylcyclopentene; *in situ* fluorination; NiMoS; Al_2O_3; silica–alumina.**

INTRODUCTION

Fluorine is widely used as an additive in hydroprocessing catalysts. Its role in Al_2O_3 catalysts and Al_2O_3-supported catalysts has been reviewed by Ghosh and Kydd (1). Recent studies have furthered the understanding of the effect of fluorine in hydrotreating catalysts (2–10). Fluorination is conventionally performed by impregnating the support with a fluoride salt, such as NH_4F (see, e.g., Refs. 3, 4). After NH_4F impregnation, drying, and calcination, molybdenum and nickel salts are introduced as usual by impregnation. After a subsequent calcination, the resulting materials are sulfided in a stream of H_2S in H_2. The disadvantage of this method is that the dispersion of MoS_2 and Ni may be different in fluorine-containing and fluorine-free NiMo catalysts. Thus, it is difficult to compare their catalytic properties. *In situ* fluorination, after preparation of the NiMo catalyst in the sulfidic form, has been described in patents (see, e.g., Refs. 11, 12), but not in the open literature. Because the metal sulfides are prepared before fluorination in this method, the catalyst dispersion might not be influenced by the fluorination. *In situ* fluorination may thus allow us to investigate the role of fluorine without having to deal with the complication of different dispersions of the metal sulfide phase in fluorine-free and fluorine-containing catalysts.

Therefore, we studied the effect of *in situ* fluorination of sulfided NiMo catalysts supported on γ-Al_2O_3 and amorphous silica–alumina (ASA) on hydrodenitrogenation (HDN). By comparing the kinetic parameters of the different catalysts, the effect of fluorination on the catalytic activity, the reaction network, and the active sites can be determined. As a model compound we chose *o*-toluidine because its HDN network contains all the reactions (hydrogenation of the aromatic ring, elimination, hydrogenation of the resulting olefin) that are essential for HDN. During the HDN of *o*-toluidine, the first intermediate, *o*-methylcyclohexylamine, is only present in minor amounts since its rate of formation is slow and its rate of elimination to the second intermediate, methylcyclohexene (MCHE), is fast. MCHE reacts relatively slowly to methylcyclohexane and is therefore always present in large amounts (13).

The hydrogenations of cyclic olefins and aromatics are important reaction steps in industrial hydroprocessing and are efficiently performed over sulfide catalysts such as NiMo and NiW supported on Al_2O_3 and ASA (14, 15). The hydrogenation of cyclic olefins plays an important role in HDN and hydrodesulfurization reaction networks and occurs on a different site on sulfide catalysts than the C–N and C–S bond cleavage reactions (16). Many studies have been devoted to the kinetics and to the mechanism of the hydrogenation of olefins over metallic catalysts (see, e.g., Refs. 17–19). Little attention has been paid, however,

[1] To whom correspondence should be addressed. Fax: 41-1-632 11 62. E-mail: prins@tech.chem.ethz.ch.

0021-9517/02 $35.00

to the catalytic chemistry and kinetics of hydrogenation reactions over sulfide catalysts.

In order to study the detailed mechanism of the HDN reaction, it is necessary to study the kinetics of the hydrogenation of MCHE separately. Because of the similarity of cyclohexene (CHE) and MCHE, we used CHE as the model compound.

EXPERIMENTAL

The catalysts, containing 4 wt% Ni and 13 wt% Mo, were prepared by pore volume impregnation of γ-Al_2O_3 (Condea) and ASA (Shell) with aqueous solution of ammonium molybdate tetrahydrate (Fluka) and nickel nitrate hexahydrate (Fluka), followed by drying at 120°C overnight and calcination at 500°C for 4 h in air after each impregnation step. The resulting NiMo/Al_2O_3 catalyst had a pore volume of 0.42 ml $\cdot$ g^{-1} and a surface area of 155 $m^2 \cdot g^{-1}$ as determined by BET nitrogen adsorption. The NiMo/ASA catalyst had a pore volume of 0.43 ml $\cdot$ g^{-1} and a surface area of 265 $m^2 \cdot g^{-1}$. An amount of 0.02–0.05 g of catalyst diluted with 8 g of SiC was loaded in a continuous-flow fixed-bed microreactor. After loading in the reactor, the catalyst was dried for 2 h at 400°C and then sulfided with a mixture of 10% H_2S in H_2 at 1.0 MPa. Sulfidation started from ambient temperature with a slow increase in 14 h to 370°C; the temperature was then maintained at 370°C for 2 h.

The *in situ* fluorination was performed after the sulfidation step. The pressure was first increased to that of the reaction condition (5.0 MPa) with the sulfiding gas. After cooling the reactor to 200°C, a solution of 0.26 wt% *o*-fluorotoluene (Fluka) in *n*-decane (Fluka) was dosed to the reactor with a syringe pump (Isco 100D). The temperature was slowly raised to 370°C and kept for 48 h, while the sulfiding and fluorination gas was flowing through the reactor. The fluorine contents in the thus-fluorinated catalysts was about 1 wt%, as determined by X-ray fluorescence absorption.

After activation, the temperature was adjusted to 350°C, and the sulfiding and fluorination gas was switched to pure hydrogen. Then a solution of CHE, octane (solvent), *n*-heptane (HEP, internal standard), and dimethyldisulfide (to generate H_2S *in situ*) (all from Fluka, without further treatment) was fed to the reactor with a high-pressure syringe pump (Isco 500D). The temperature range studied was between 310 and 350°C. Partial pressures at the reactor inlet were $P_{CHE} = 16, 60$, or 100 kPa, $P_{HEP} = 0.1$ kPa, $P_{H_2S} = 17.5$ kPa, $P_{H_2} = 4.8$ MPa, and octane as the balance. The liquid feed rate was varied between 0.039 and 0.50 ml $\cdot$ min^{-1}.

The reaction products were analyzed by online gas chromatography on a Varian Star 3400CX instrument equipped with a 30 m DB-5MS fused silica capillary column and a flame ionization detector. Kinetic data were obtained by varying the weight time and reactant initial partial pressure after stabilization for 20 h. Weight time was defined as $\tau = m_C/n_{feed,total}$, where m_C denotes the catalyst weight and $n_{feed,total}$ the total molar flow fed to the reactor. The hydrogen flow rates were always changed in proportion to the liquid flow rates. No diffusion and transport limitations were detected under the conditions studied. This allowed us to model the reaction with a Langmuir–Hinshelwood mechanism using nonlinear numeric fitting of the data with the SCIENTIST programme from MicroMath Inc. The goodness-of-fit is indicated by the model selection criterion (MSC) and is defined by the formula

$$\mathrm{MSC} = \ln\left(\frac{\sum_{i=1}^{n} w_i (Y_{obs_i} - \bar{Y}_{obs})^2}{\sum_{i=1}^{n} w_i (Y_{obs_i} - Y_{cal_i})^2}\right) - \frac{2p}{n},$$

where $\bar{Y}_{obs}$ is the weighted mean of the observed data Y_{obs_i}, Y_{cal_i} is calculated data, p and n are the number of parameters and the measured points in the model, respectively, and w_i is the weight applied to the points. All the weight factors were taken to be equal to 1 in our fitting. The larger the value of MSC, the better the fit.

RESULTS

Hydrogenation of CHE

The reaction network for the hydrogenation of CHE is shown in Fig. 1. Over the NiMo/Al_2O_3 catalyst, the main product of the hydrogenation of CHE was cyclohexane (CH), as shown in the product distribution versus weight time plot in Fig. 2a. Two types of skeletal-isomerization products were observed, i.e., methylcyclopentenes

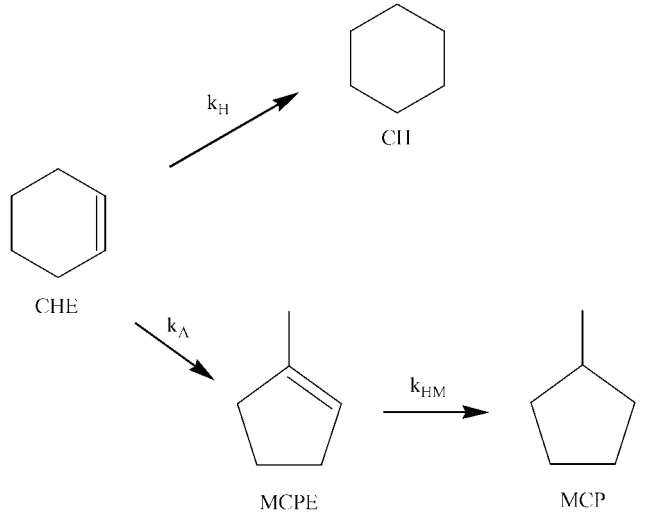

FIG. 1. Reaction scheme for the hydrogenation of cyclohexene (CHE) to cyclohexane (CH) and for the isomerization of CHE to methylcyclopentene (MCPE) and its subsequent hydrogenation to methylcyclopentane (MCP) over sulfided NiMo/Al_2O_3 and NiMo/ASA catalysts.

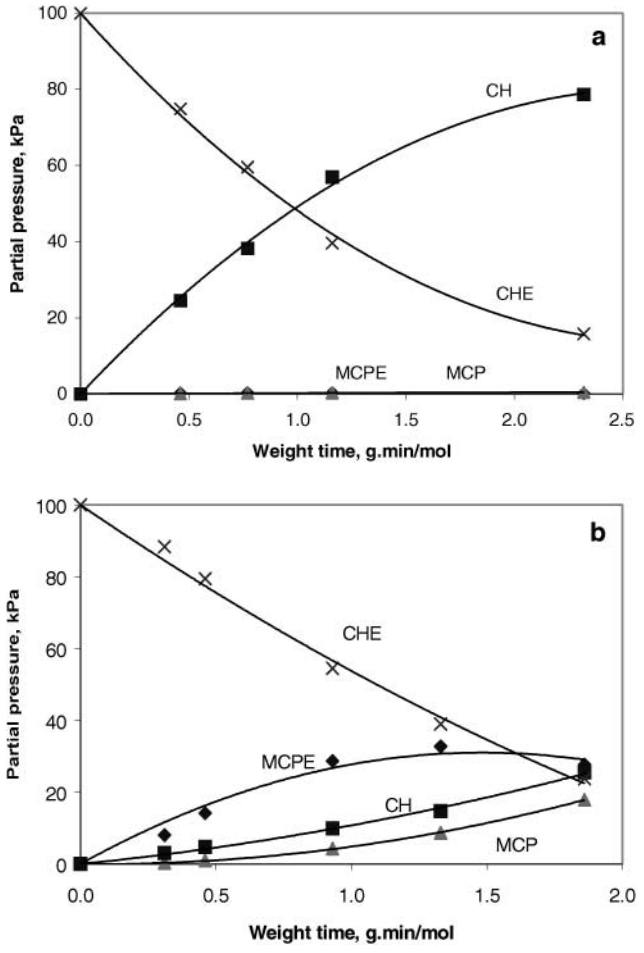

FIG. 2. Product distribution during the hydrogenation of cyclohexene (CHE) to cyclohexane (CH) and the isomerization to methylcyclopentene (MCPE) and methylcyclopentane (MCP) at 350°C over (a) $NiMo/Al_2O_3$ and (b) NiMo/ASA.

(MCPEs) and methylcyclopentane (MCP), which is formed by successive hydrogenation of MCPE. The conversion to these isomerization products was always less than 1% over $NiMo/Al_2O_3$, but reached 15% for the fluorinated $NiMo/Al_2O_3$ catalyst ($F–NiMo/Al_2O_3$). A trace of cyclohexanethiol was detected at the lowest temperature used (310°C) over the fluorinated catalysts, in agreement with Van Gestel *et al*., who observed up to 10% cyclohexanethiol at 280°C and 4.0 MPa over a sulfided $NiMo/Al_2O_3$ catalyst (20).

More isomerization products, MCPEs and MCP, were formed over the NiMo/ASA catalyst than over the $NiMo/Al_2O_3$ catalyst. Substantial amounts of 3-MCPE and 4-MCPE were detected in addition to 1-MCPE and MCP. The product distribution versus weight time plot for the NiMo/ASA catalyst shows clearly that MCPE is an intermediate and that MCP is the final product (Fig. 2b). After fluorination of the ASA-supported catalyst, the yield of isomerization products was even higher and attributed up to 75% of the products. No cracking products were observed under our reaction conditions.

To study the active sites for the hydrogenation of CHE, pure CHE without dimethyl disulfide was fed to the reactor as well. In the absence of H_2S the hydrogenation of CHE was much faster than in the presence of H_2S (Fig. 3). The strong inhibition effect of H_2S on the olefin hydrogenation indicates that the active sites for the hydrogenation of CHE are surface sites with low sulfur coordination, i.e., vacancies on which H_2S as well as an olefin can competitively adsorb. This is in agreement with earlier findings (2, 5, 21–23). Further evidence was provided by Hubaut *et al*. (24) by reducing MoS_2/Al_2O_3 catalysts at different temperatures. They obtained the best activity for the hydrogenation of olefins when a large number of anionic vacancies was created.

The plot of $-\ln(1-x)$ versus weight time shows that the hydrogenation of CHE is not a first-order reaction on $NiMo/Al_2O_3$ catalysts at the initial partial pressures of CHE that we applied. Not only at 310°C but also at 350°C the plot is not linear (Fig. 4a). The same holds for the fluorinated catalyst (not shown) and for the NiMo/ASA catalysts (Fig. 4b). It is clear that under our reaction conditions the reaction is between first and zero order.

The effect of the support on the hydrogenation of CHE is shown in Fig. 5. The Al_2O_3-supported NiMo catalyst has a higher conversion (hydrogenation, as well as total) than the ASA-supported catalyst. On the other hand, the yield of isomerization products (MCPEs + MCP) is higher on the ASA-supported catalyst owing to its higher acidity.

The *in situ* fluorination was performed after the metal compounds had been transformed to their sulfided states. The fluorination precursor *o*-fluorotoluene can be

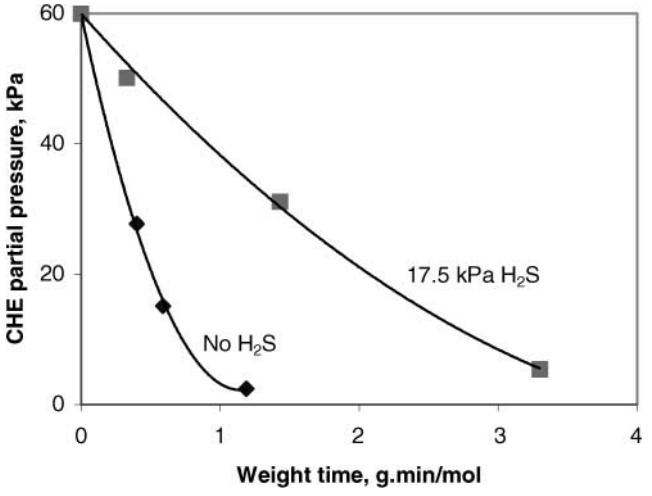

FIG. 3. Inhibition of H_2S on the hydrogenation of cyclohexene (CHE) over NiMo/ASA at 350°C.

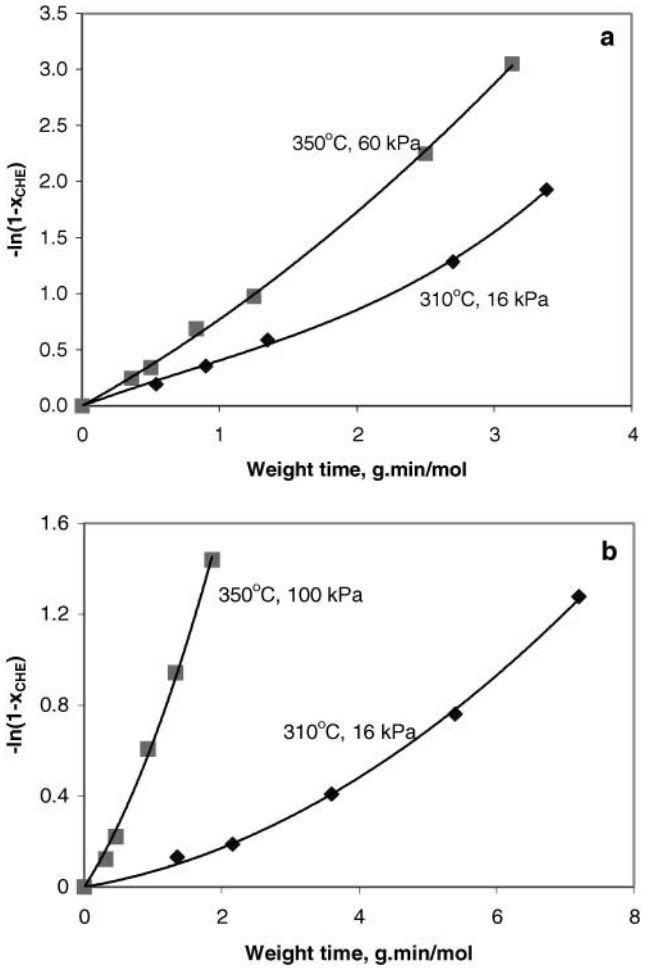

FIG. 4. Plot of $-\ln(1 - x_{CHE})$ versus weight time for the hydrogenation of cyclohexene (CHE) over (a) $NiMo/Al_2O_3$ and (b) NiMo/ASA.

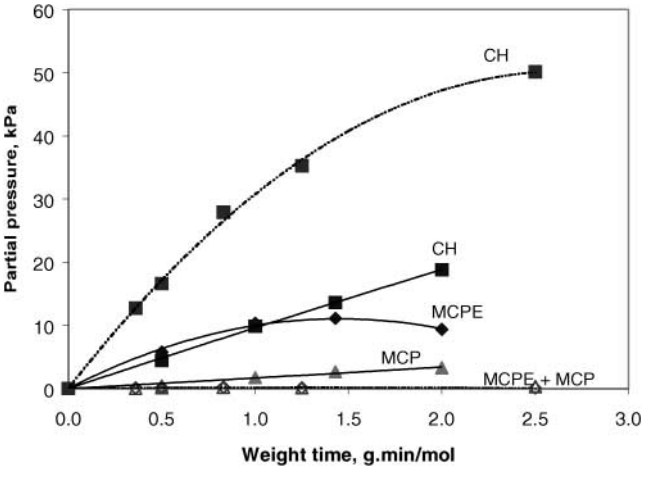

FIG. 5. Conversion of cyclohexene to cyclohexane (CH) and methylcyclopentene (MCPE) and methylcyclopentane (MCP) over $NiMo/Al_2O_3$ (dashed lines) and NiMo/ASA (solid lines) at 330°C.

decomposed to HF and toluene over sulfided catalysts, while the toluene is not further hydrogenated under these conditions (33). The HF formed acts as the real fluorination agent.

Fluorination has a positive effect on the conversion of CHE over the Al_2O_3-supported catalyst as well as over its ASA-supported counterparts. A detailed analysis of the products shows, however, that this positive effect is not due to an increased hydrogenation. For both series of catalysts, the conversion to CH stays constant; only the isomerization to MCPE and MCP increases substantially after fluorination (Figs. 6a and 6b). This is due to the higher acidity introduced into the catalysts by fluorination, which promotes the isomerization reaction.

Hydrogenation of 1-Methylcyclopentene

When MCPE and MCP are present in large amounts on ASA-supported catalysts, it was impossible to obtain a good

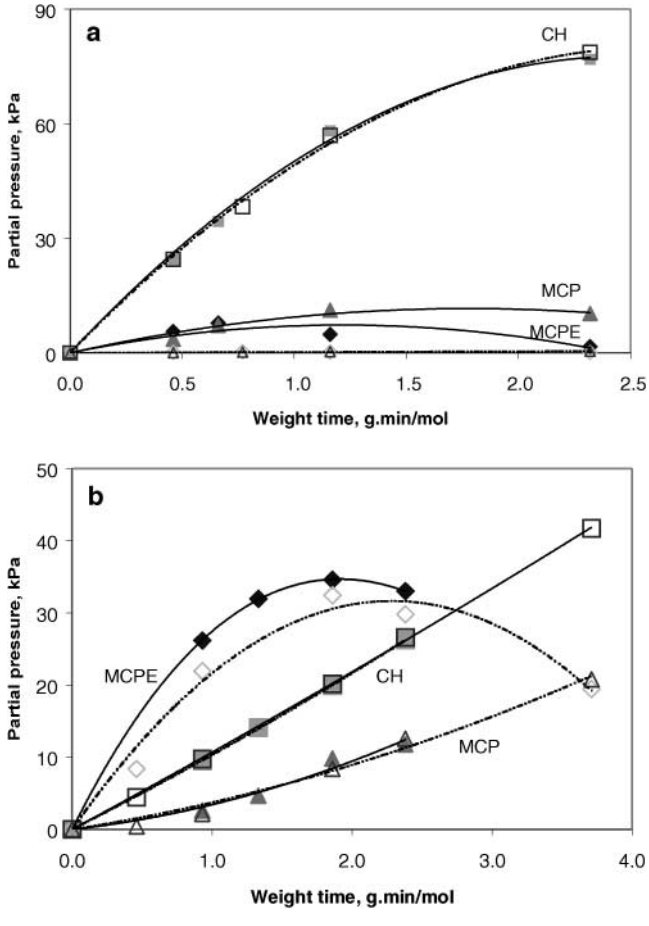

FIG. 6. Fluorination effect on the conversion of 100 kPa cyclohexene to cyclohexane (CH), methylcyclopentene (MCPE), and methylcyclopentane (MCP) at 350°C over (a) $NiMo/Al_2O_3$ and (b) NiMo/ASA. Solid lines for fluorinated catalysts, dashed lines for fluorine-free catalysts.

fit of the CHE reaction when leaving out the contribution from MCPEs and MCP. Therefore, we studied the hydrogenation of 1-MCPE separately to complete the whole reaction network of the CHE reaction (Fig. 1). The reaction conditions for the hydrogenation of 1-MCPE were the same as those for the hydrogenation of CHE. The hydrogenation of 1-MCPE was studied at two initial partial pressures of 1-MCPE, 16 and 100 kPa. Only the NiMo/ASA and F–NiMo/ASA catalysts were studied, because the formation of MCPE and MCP in the conversion of CHE was only substantial over these catalysts.

When 1-MCPE was fed over NiMo/ASA, the saturated product MCP was formed readily (Fig. 7). In addition, substantial amounts of 3-MCPE and 4-MCPE were detected, indicating that isomerization (double bond shift) took place on the ASA-supported catalysts. The amount of CHE formed by skeletal isomerization of the MCPEs plus the CH formed by the successive hydrogenation of CHE was always less than 5%, even on the fluorinated NiMo/ASA catalyst, which has the highest acidity. No cracking products, with a carbon number below 6, were formed up to 400°C. These results indicate that the reverse reaction from MCPE to CHE can be neglected in the CHE reaction network (Fig. 1).

The fast disappearance of 1-MCPE and evolution of 3-MCPE and 4-MCPE at short weight time (cf. Fig. 7) suggest that 3-MCPE and 4-MCPE are intermediates in the conversion of 1-MCPE. The reaction scheme for 1-MCPE conversion is shown in Fig. 8. The isomerization of 1-MCPE to 3-MCPE and 4-MCPE occurs on the acid sites, while the hydrogenation of MCPE takes place on the hydrogenation sites. This reaction scheme gives a good fit with the reaction data (Fig. 9). Fitting based on this scheme generated large uncertainties in the kinetic parameters but clearly demonstrated that the transformation of 1-MCPE

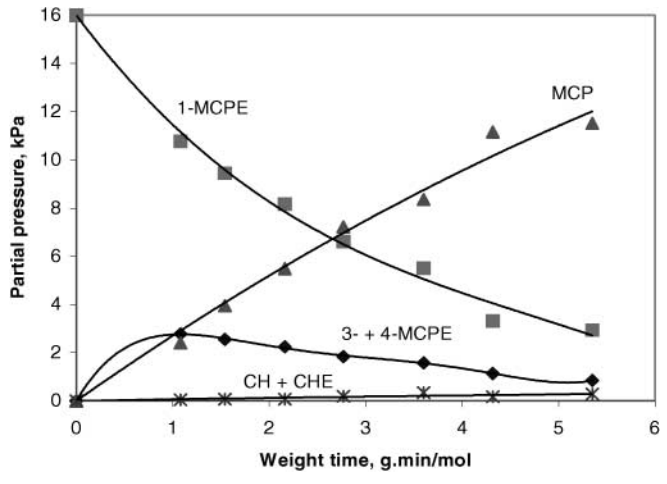

FIG. 7. Product distribution during the hydrogenation of 1-methylcyclopentene (MCPE) over NiMo/ASA at 350°C and 16 kPa.

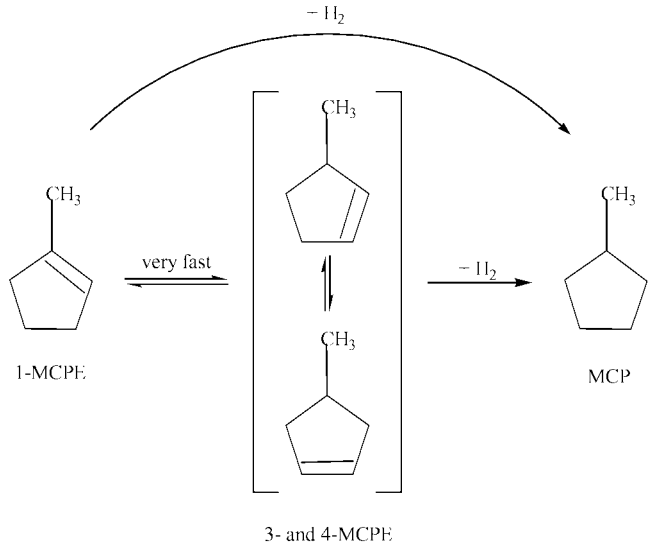

FIG. 8. Reaction scheme for the conversion of 1-methylcyclopentene (1-MCPE) to 3-methylcyclopentene (3-MCPE) and 4-methylcyclopentene (4-MCPE), and then to methylcyclopentane (MCP) over NiMo/ASA catalysts.

to 3-MCPE and 4-MCPE is very fast. The enthalpy of reaction from 1-MCPE to 3-MCPE and 4-MCPE is about 8 and 7.5 kJ · mol^{-1}, respectively (38), and 1-MCPE isomerizes quickly to 3- and 4-MCPE under our reaction conditions. Because we are more interested in the parameters for the hydrogenation than for the isomerization of 1-MCPE, we decided to lump the three MCPE isomers together when fitting the hydrogenation reaction of 1-MCPE. Thus, the fitting of the kinetics of the hydrogenation of 1-MCPE was

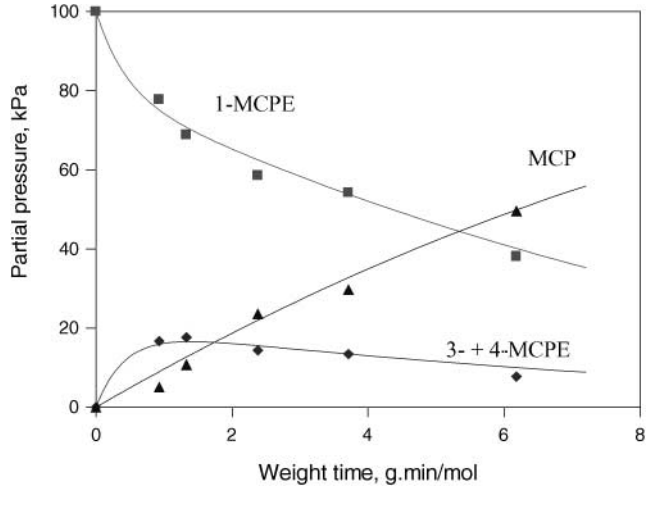

FIG. 9. A fit of the conversion of 100 kPa 1-methylcyclopentene (1-MCPE) to 3-methylcyclopentene (3-MCPE) and 4-methylcyclopentene (4-MCPE), and then to methylcyclopentane (MCP), including the route from 1-MCPE directly to MCP over F–NiMo/ASA at 350°C. Lines are the fitted results and points are the experimental data.

based on the Langmuir–Hinshelwood equation,

$$\frac{dP_{\mathrm{MCP}}}{d\tau} = -\frac{dP_{\mathrm{MCPE}}}{d\tau} = \frac{k_{HM}K_{HM}P_{\mathrm{MCPE}}}{1 + K_{HM}P_{\mathrm{MCPE}}} \qquad [1]$$

where k_{HM} and K_{HM} are the rate and adsorption equilibrium constants for MCPE on the hydrogenation sites, respectively, and P_{MCPE} is the sum of the partial pressures of the three MCPE isomers. As an example of the goodness of the fit, the experimental results and the fits of the hydrogenation of 16 and 100 kPa MCPE to MCP over F–NiMo/ASA at 350°C are presented in Fig. 10. The resulting parameters for the hydrogenation of 1-MCPE are shown in Table 1.

Kinetics of the Hydrogenation of CHE

Kinetic modeling for the hydrogenation of CHE was performed based on the reaction scheme shown in Fig. 1. Since MCPE and MCP were hardly detected over the Al_2O_3-supported catalyst, we did not consider the isomerization for the kinetic modeling for this catalyst and only equation [2] was used:

$$\frac{dP_{\mathrm{CH}}}{d\tau} = -\frac{dP_{\mathrm{CHE}}}{d\tau} = \frac{k_H K_H P_{\mathrm{CHE}}}{1 + K_H P_{\mathrm{CHE}}}. \qquad [2]$$

For the F–NiMo/Al_2O_3 catalyst at 350°C and for the NiMo/ASA and F–NiMo/ASA catalysts at all temperatures, MCPE and MCP were present in substantial amounts and we had to use the whole network. The back reaction from MCPE to CHE was not taken into account, since the results presented in the foregoing section showed that this reaction could be neglected under our conditions. There are different kinds of sites for the hydrogenation (H-sites) and isomerization (A-sites) of CHE. Since MCPE and CHE can be adsorbed on both kinds of sites, Eqs. [3]–[6] are obtained:

$$-\frac{dP_{\mathrm{CHE}}}{d\tau} = \frac{k_H K_H P_{\mathrm{CHE}}}{1 + K_H P_{\mathrm{CHE}} + K_{HM} P_{\mathrm{MCPE}}} + \frac{k_A K_A P_{\mathrm{CHE}}}{1 + K_A P_{\mathrm{CHE}} + K_A P_{\mathrm{MCPE}}}, \qquad [3]$$

$$\frac{dP_{\mathrm{CH}}}{d\tau} = \frac{k_H K_H P_{\mathrm{CHE}}}{1 + K_H P_{\mathrm{CHE}} + K_{HM} P_{\mathrm{MCPE}}}, \qquad [4]$$

$$\frac{dP_{\mathrm{MCPE}}}{d\tau} = \frac{k_A K_A P_{\mathrm{CHE}}}{1 + K_A P_{\mathrm{CHE}} + K_A P_{\mathrm{MCPE}}} - \frac{k_{HM} K_{HM} P_{\mathrm{MCPE}}}{1 + K_H P_{\mathrm{CHE}} + K_{HM} P_{\mathrm{MCPE}}}, \qquad [5]$$

$$\frac{dP_{\mathrm{MCP}}}{d\tau} = \frac{k_{HM} K_{HM} P_{\mathrm{MCPE}}}{1 + K_H P_{\mathrm{CHE}} + K_{HM} P_{\mathrm{MCPE}}}. \qquad [6]$$

In these equations, k_H, k_A, and k_{HM} are the reaction rate constants for the CHE hydrogenation, CHE isomerization, and MCPEs (sum of three isomers) hydrogenation, respectively, while K_H, K_A, and K_{HM} are the corresponding adsorption equilibrium constants. P_{CH}, P_{CHE}, P_{MCPE}, and P_{MCP} are the partial pressures of CH, CHE, MCPEs, and MCP, respectively. We assume that the adsorption equilibrium constants of all MCPEs and CHE on the isomerization sites are equal. A separate experiment showed no influence from adding CH on the conversion of CHE. This indicates that MCP and CH are very weakly adsorbed on the hydrogenation and isomerization sites compared with MCPE and CHE. The values of the rate and adsorption equilibrium constants (k_{HM} and K_{HM}), determined in the previous section from the hydrogenation of 1-MCPE, were used in the fitting of the CHE results on the ASA-supported catalysts. The hydrogen partial pressure was always kept constant in our system and was, therefore, combined with the rate constant k.

TABLE 1

Fitted Parameters for MCPE Hydrogenation on NiMo/ASA Catalysts[a]

Catalyst	k_{HM} (kPa · mol · g^{-1} · min^{-1})	K_{HM} (kPa^{-1})	MSC
NiMo/ASA			
310°C	4.5 (0.6)	0.023 (0.010)	5.2
330°C	10 (1.3)	0.017 (0.005)	5.7
350°C	31 (6.8)	0.008 (0.003)	5.1
F–NiMo/ASA			
310°C	2.7 (0.4)	0.013 (0.004)	8.3
330°C	8.4 (0.3)	0.010 (0.003)	6.4
350°C	27 (9.6)	0.006 (0.003)	5.4

[a] Standard deviation in parentheses.

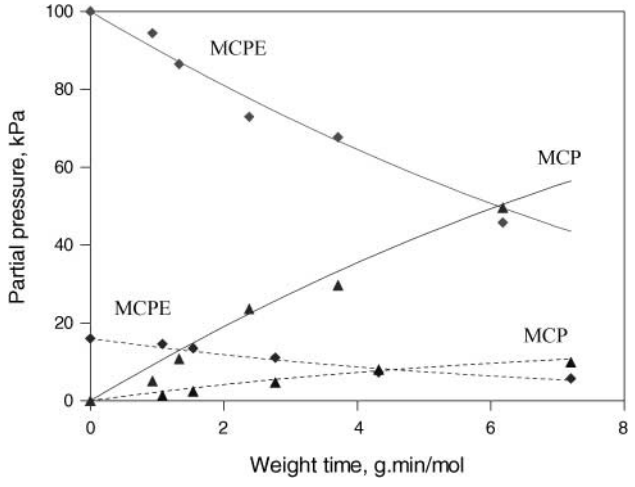

FIG. 10. Fit of the hydrogenation of the sum of all methylcyclopentenes (MCPE) to methylcyclopentane (MCP) over F–NiMo/ASA at 350°C. Lines are the fitted results and points are the experimental data.

TABLE 2

Fitted Parameters for CHE Hydrogenation on $NiMo/Al_2O_3$ Catalysts[a]

Catalyst	k_H (kPa · mol · g^{-1} · min^{-1})	K_H (kPa^{-1})	MSC
$NiMo/Al_2O_3$			
310°C	23 (1.1)	0.024 (0.002)	5.9
330°C	80 (7.0)	0.008 (0.001)	6.3
350°C	296 (69)	0.003 (0.001)	6.1
F–$NiMo/Al_2O_3$			
310°C	20 (1.7)	0.032 (0.007)	4.7
330°C	59 (9.4)	0.014 (0.004)	4.6
350°C	248 (91)	0.004 (0.002)	4.6

[a] Standard deviation in parentheses.

All reactions were performed at a total pressure of 5.0 MPa and a partial pressure of hydrogen at the reactor inlet of 4.8 MPa. The kinetic data were obtained after 20 h on stream when the catalyst had reached a stable activity at 350°C. No deactivation was observed during the experiments. Three initial partial pressures of CHE were used at each temperature with varying weight times in order to achieve a wide range of CHE conversions. More than four weight times (liquid flow rates range from 0.025 to 0.5 ml · min^{-1}) were tested at each CHE initial partial pressure. The temperatures studied were 310, 330, and 350°C. Based on the thus-obtained data, kinetic modeling was performed using the SCIENTIST® program. Reaction rate constants and adsorption constants for different reaction steps on various sites were obtained from the fitting and are presented in Tables 2 and 3. An example of the fit is shown in Fig. 11.

DISCUSSION

Our results shows that at a CHE initial partial pressure between 16 and 100 kPa, at a H_2S partial pressure of 17.5 kPa, and between 310 and 350°C, the hydrogenation is between zero and first order in CHE over sulfided NiMo catalysts. In the literature, first-order kinetics has been reported for the hydrogenation of olefins over sulfided catalysts, but these results were obtained at much lower olefin partial pressures than in our experiments (16, 25, 26). Nag *et al*. (27) observed that the hydrogenation of CHE is zero order with respect to CHE (up to 18 kPa), and first order to hydrogen (up to 80 kPa) on a sulfided NiW/Al_2O_3 catalyst at atmospheric pressure and between 250 and 350°C. Günther (28) studied the kinetics of olefin hydrogenation over a WS_2–NiS catalyst. He found that in the hydrogenation of a mixture of olefins with a boiling point between 50 and 150°C, the reaction is pseudo first order with respect to olefins and that the reaction rate is practically independent of the hydrogen pressure in the range 5 to 30 MPa. This agrees with observations by Heinemann *et al*. in a study of the hydrogenation of heptenes on a sulfided Co–Mo catalyst (29).

The ASA-supported catalysts have a much lower hydrogenation activity for olefins (factor between 5 and 9) than do their Al_2O_3-supported counterparts (cf. Fig. 5). This lower hydrogenation activity is in contrast to our observation that ASA-supported catalysts have a higher HDN activity than their Al_2O_3-supported counterparts (30). The decreased olefin hydrogenation on the ASA-supported catalyst may be due to the difference between the two supports. Although the ASA support has a higher surface area than Al_2O_3, part of it consists of SiO_2 domains, and the other part of Al_2O_3 domains. It has been reported that Al_2O_3 adsorbs Mo species stronger than silica, regardless of the pH used during preparation (31, 32). Consequently, more Mo will be accommodated on the alumina domains than on silica domains during catalyst preparation on ASA. Our ASA support contains only 25% Al_2O_3, however, on which most of the Mo species will adsorb. This leads to a lower dispersion of the metal sulfides on the ASA support and thus to a lower hydrogenation activity of CHE, especially when the metal loading is relatively high.

TABLE 3

Fitted Parameters for CHE Reaction on NiMo/ASA Catalysts[a]

Catalyst	k_H (kPa · mol · g^{-1} · min^{-1})	K_H (kPa^{-1})	k_A (kPa · mol · g^{-1} · min^{-1})	K_A (kPa^{-1})	MSC
NiMo/ASA					
310°C	4.5 (0.4)	0.035 (0.009)	0.9 (0.2)	0.070 (0.090)	5.5
330°C	12 (1.2)	0.026 (0.006)	28 (11)	0.003 (0.003)	5.1
350°C	36 (1.8)	0.001 (0.001)	221 (31)	0.001 (0.001)	4.8
F–NiMo/ASA					
310°C	3.7 (0.2)	0.110 (0.034)	1.3 (0.4)	0.050 (0.050)	5.4
330°C	9.5 (0.7)	0.060 (0.018)	56 (14)	0.002 (0.001)	4.9
350°C	29 (1.6)	0.015 (0.009)	301 (38)	0.001 (0.001)	4.5

[a] Standard deviation in parentheses.

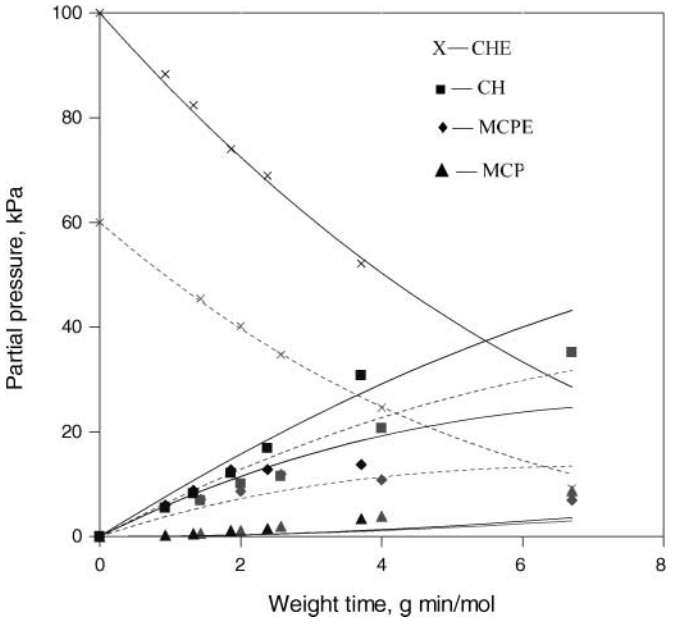

FIG. 11. Fit of the hydrogenation of 100 and 60 kPa cyclohexene (CHE) to cyclohexane (CH) and isomerization to methylcyclopentenes (MCPE) and methylcyclopentane (MCP) over NiMo/ASA at 330° C. Lines are the fitted results and points are the experimental data.

A promoting effect of fluorine on the conversion of olefins has been reported for Al_2O_3-supported NiMo and CoMo catalysts in which the fluorine was introduced by *ex situ* fluorination (2, 5, 7). Ramirez *et al.* (5) showed that fluorine increased the activity for the hydrogenation of olefin and ascribed the promotion to the increased catalyst dispersion by fluorine incorporation. Papadopoulou *et al.* (34, 35) concluded that, during the activitation process, fluorine ions hinder the reduction and/or sulfidation of Mo^{VI}- and the sulfidation of Ni^{II}-supported ions of the $NiMo/Al_2O_3$ catalyst after *ex situ* fluorination. Other studies proved just the opposite: that fluorine promotes the degree of sulfidation (3, 36). Van Veen *et al*. (37) explained the role of fluorination by a transformation of the partly sulfided NiMoS phase to the more active, fully sulfided NiMoS phase. After breaking the Mo–O–Al linkage with the support, the NiMoS phase interacts with the support only via van der Waals forces. This may lead to increased stacking of the MoS_2 slabs and thus to a better accessibility of the sites for the adsorbent and to a higher activity.

Our results demonstrate that *in situ* fluorination does not influence the hydrogenation of olefins at all. In all cases the yield of CH did not change upon fluorination (Fig. 6). Only the acid-catalyzed isomerization of CHE to MCPE was promoted substantially on the Al_2O_3-supported catalyst and slightly on the ASA-supported catalyst. Table 2 shows that the fluorination does not influence the hydrogenation rate constants very much over $NiMo/Al_2O_3$. The equilibrium adsorption constants of CHE on the hydrogenation sites

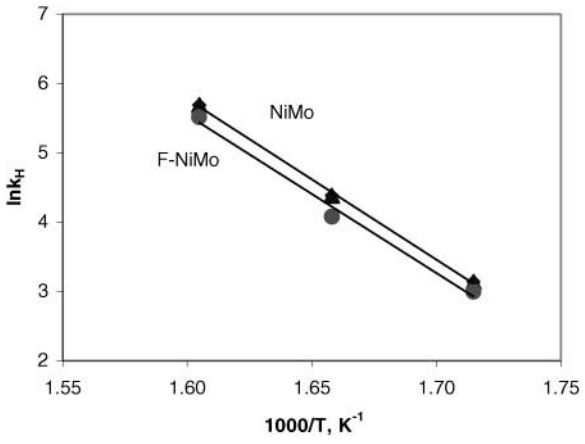

FIG. 12. Plot of $\ln k_H$ versus $1/T$ for the hydrogenation of cyclohexene over $NiMo/Al_2O_3$ and $F–NiMo/Al_2O_3$.

seem to increase after fluorination, which would mean a stronger adsorption of CHE on the fluorinated catalyst. As a result, the amount of CH formed in the system remains unchanged (Fig. 6a). More isomerization products are formed with the fluorinated catalyst, leading to a smaller MSC in the model fitting (Table 2).

The reaction rate constants for the hydrogenation of CHE to CH over the ASA-supported catalysts decrease slightly after fluorination, while the adsorption equilibrium constants of CHE on the hydrogenation sites seem to increase with fluorination (Table 3), as in the case of the Al_2O_3-supported catalysts. Although the parameters for the isomerization were obtained with large standard deviations, it is nevertheless clear that the rate constants increase after fluorination, while the adsorption equilibrium constants of CHE on the acid sites remain more or less the same.

From the results obtained at different temperatures, one can calculate the temperature dependence of the

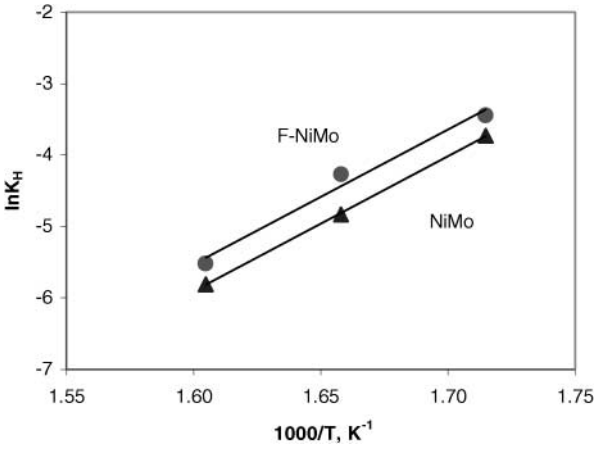

FIG. 13. Plot of $\ln K_H$ versus $1/T$ for the hydrogenation of cyclohexene over $NiMo/Al_2O_3$ and $F–NiMo/Al_2O_3$.

TABLE 4

Temperature Dependence of k and K[a]

Catalyst	$NiMo/Al_2O_3$	$F–NiMo/Al_2O_3$	NiMo/ASA	F–NiMo/ASA
E_H ($kJ \cdot mol^{-1}$)	193 (15)	190 (15)	157 (15)	155 (11)
k_{H0} ($kPa \cdot mol \cdot g^{-1} \cdot min^{-1}$)	4×10^{18}	2×10^{18}	5×10^{14}	3×10^{14}
$-\Delta H_H$ ($kJ \cdot mol^{-1}$)	157 (37)	157 (37)	100 (44)	150 (28)
K_{H0} (kPa^{-1})	2×10^{-16}	3×10^{-16}	4×10^{-11}	5×10^{-15}
E_A ($kJ \cdot mol^{-1}$)	—	—	416 (30)	413 (30)
k_{A0} ($kPa \cdot mol \cdot g^{-1} \cdot min^{-1}$)	—	—	2×10^{37}	2×10^{37}

[a] Standard deviation in parentheses.

reaction rate and adsorption equilibrium constants. The activation energies of the hydrogenation reaction were calculated according to the Arrhenius plot of ln k versus $1/T$ ($k = k_0 e^{-E/RT}$) for the Al_2O_3-supported catalysts (Fig. 12). Similarly, the heats of adsorption were obtained from $K = K_0 e^{-\Delta H/RT}$ (Fig. 13). Table 4 shows that the fluorinated $NiMo/Al_2O_3$ catalyst has the same activation energy for the hydrogenation of CHE to CH as the $NiMo/Al_2O_3$ catalyst. Also the heat of adsorption was found to be the same for the fluorinated and unfluorinated $NiMo/Al_2O_3$ catalysts. Similar results were found for the NiMo/ASA and the fluorinated NiMo/ASA catalysts (Table 4). The activation energy for the isomerization reaction was not changed after fluorination. This suggests that the surface sites of NiMo/ASA were not modified for the isomerization reaction after fluorination. The improved activity can be attributed to an increase in the number of acid sites introduced by the *in situ* fluorination, which was caused by the higher electronegativity of fluorine linked to aluminium. This in turn enhances the isomerization reaction.

Our results show that *in situ* fluorination hardly influences the properties of the sulfided NiMo catalysts for the hydrogenation of olefins. That the sites stay the same is not surprising, since it is known that fluorine is positioned on the support and not on the metal sulfide (36). The fluorine on the support improves the acidity of the catalyst, which explains that its main effect on the reaction of CHE is on isomerization and not hydrogenation. The fact that hydrogenation activity is not influenced means that the number of sites did not change by *in situ* fluorination. Promoted MoS_2 catalysts consist of two-dimensional MoS_2 particles with nickel atoms decorating the edges. Vacancies on the edges are supposed to be the active sites. It is actually assumed that the hydrogenation of olefins on MoS_2 and promoted MoS_2 is not structure sensitive, meaning that any vacancy will be active and that vacancies on the top platelets of a stack of $Ni–MoS_2$ particles are not more active than vacancies on the underlying ones. In that case, the insensitivity of the olefin hydrogenation to the presence of fluorine indicates that the *in situ* fluorination did not change the size of the $Ni–MoS_2$ particles. It is impossible, however, to draw any conclusion about a change in the degree of stacking of the $Ni–MoS_2$ platelets.

CONCLUSIONS

The hydrogenation of CHE takes place on sulfur-deficient sites of sulfided NiMo catalysts. The Al_2O_3-supported catalysts exhibit a higher activity than their ASA-supported counterparts, which is probably due to the better dispersion of Mo on the Al_2O_3 support. Over NiMo/ASA catalysts, the reaction network is different from $NiMo/Al_2O_3$ catalysts and more isomerization products are formed. Lower rate constants and higher adsorption equilibrium constants for the hydrogenation of CHE were found for the fluorinated catalysts, resulting in an unchanged conversion of CHE to CH. The activation energy for the isomerization stays constant. *In situ* fluorination introduced more acid sites for the isomerization reaction over both the Al_2O_3- and ASA-supported sulfided NiMo catalysts.

REFERENCES

1. Ghosh, A. K., and Kydd, R. A., *Catal. Rev.–Sci. Eng*. **27**, 539 (1985), and references therein.
2. Jirátová, K., and Kraus, M., *Appl. Catal*. **27**, 21 (1986).
3. Benitez, A., Ramirez, J., Vazquez, A., Acosta, D., and Lopez Agudo, A., *Appl. Catal. A* **133**, 103 (1995).
4. Benitez, A., Ramirez, J., Cruz-Reyes, J., and Lopez Agudo, A., *J. Catal.* **172**, 137 (1997).
5. Ramirez, J., Cuevas, R., Lopez Agudo, A., Mendioroz, S., and Fierro, J. L. G., *Appl. Catal*. **57**, 223 (1990).
6. Qu, L., Jian, M., Shi, Y., and Li, D., *Chin. J. Catal.* **19**, 608 (1998).
7. Fierro, J. L. G., Cuevas, R., Ramirez, J., and Lopez Agudo, A., *Bull. Soc. Chim. Belg*. **100**, 945 (1991).
8. Lewandowski, M., and Sarbak, Z., *Appl. Catal. A* **156**, 181 (1997).
9. Kwak, C., Kim, M. Y., Song, C. J., and Moon, S. H., *Stud. Surf. Sci. Catal.* **121**, 283 (1999).
10. Kwak, C., and Moon, S. H., *Korean J. Chem. Eng*. **16**, 608 (1999).
11. Ladeur, P., Post, B., Fagot, M., and Saint, J. P., U.K. Patent GB 2,024,642 (1980).
12. Bertolacini, R. J., Mosby, J. F., and Schwartz, J. G., U.S. Patent 4,420,388 (1983).
13. Rota, F., and Prins, R., *Stud. Surf. Sci. Catal*. **127**, 319 (1999).
14. Weisser, O., and Landa, S., "Sulphide Catalysts, Their Properties and Applications." Pergamon Press, New York, 1973.

15. Girgis, M. J., and Gates, B. C., *Ind. Eng. Chem. Res*. **30**, 2021 (1991).
16. Jian, M., and Prins, R., *Catal. Lett.* **50**, 9 (1998).
17. Segal, E., Madon, R. J., and Boudart, M., *J. Catal*. **52**, 45 (1978).
18. Gonzo, E. E., and Boudart, M., *J. Catal*. **52**, 462 (1978).
19. Marques da Cruz, G., Bugli, G., and Djega-Mariadassou, G., *Appl. Catal*. **46**, 131 (1989).
20. Van Gestel, J., Finot, L., Leglise, J., and Duchet, J. C., *Bull. Soc. Chim. Belg*. **104**, 189 (1995).
21. Voorhoeve, R. J. H., and Stuiver, J. C. M., *J. Catal*. **23**, 228 (1971).
22. Voorhoeve, R. J. H., *J. Catal*. **23**, 236 (1971).
23. Vyskočil, V., and Kraus, M., *Collect. Czech. Chem. Commun*. **44**, 3676 (1979).
24. Hubaut, R., Poulet, O., Kasztelan, S., and Grimblot, J., *J. Mol. Catal*. **81**, 301 (1993).
25. Jian, M., and Prins, R., *Ind. Eng. Chem. Res*. **37**, 834 (1998).
26. Quartararo, J., Mignard, S., and Kasztelan, S., *J. Catal*. **192**, 307 (2000).
27. Nag, N. K., Mahipal Reddy, B., Chary, K. V. R., and Subrahmanyam, V. S., *React. Kinet. Catal. Lett.* **27**, 125 (1985).
28. Günther, G., *Chem. Technol*. **12**, 181 (1960).
29. Heinemann, H., William Kirsch, F., and Burtis, T. A., *Erdöl Kohle* **10**, 225 (1957).
30. Qu, L., and Prins, R., submitted for publication.
31. Fransen, T., Van Berge, P. C., and Mars, P., *in* "Preparation of Catalysts" (B. Delmon, P. A. Jacobs, and G. Poncelet, Eds.), p. 405. Elsevier, Amsterdam, 1976.
32. Wang, L., and Hall, W. K., *J. Catal*. **77**, 232 (1982).
33. Moreau, C., Aubert, C., Durand, R., Zmimita, N., and Geneste, P., *Catal. Today* **4**, 117 (1988).
34. Papadopoulou, C., Lycourghiotis, A., Grange, P., and Delmon, B., *Appl. Catal*. **38**, 273 (1988).
35. Papadopoulou, C., Matralis, H., Lycourghiotis, A., Grange, P., and Delmon, B., *J. Chem. Soc., Faraday Trans.* **89**, 3157 (1993).
36. Benitez, A., Ramirez, J., Fierro, J. L. G., and Lopez Agudo, A., *Appl. Catal*. **144**, 343 (1996).
37. Van Veen, J. A. R., Colijn, H. A., Hendriks, P. A. J. M., and van Welsenes, A. J., *Fuel Process. Technol*. **35**, 137 (1993).
38. NIST Chemistry WebBook, NIST Standard Reference Database Number **69**, February 2000.